

Long-term neutrino emission from a core-collapse supernova with axion-photon coupling

Masamitsu Mori*

National Institute of Technology, Numazu College, Numazu, Shizuoka 410-8501, Japan

Kanji Mori

*National Astronomical Observatory of Japan,
2-21-1 Osawa, Mitaka, Tokyo 181-8588, Japan*

(Dated: September 9, 2025)

We perform long-term general-relativistic neutrino-radiation hydrodynamic simulations for core-collapse supernovae (CCSNe) which include the cooling effect induced by the coupling between axion-like particles (ALPs) and photons. We take into account the photon coalescence and the Primakoff effect, and investigate ALPs with the mass of 10 MeV and the coupling constant $g_{a\gamma}$ of $1.0 \times 10^{-9} \text{ GeV}^{-1}$ to $7.0 \times 10^{-9} \text{ GeV}^{-1}$. It is found that the effects of the ALP cooling emerge in the late phase rather than the early phase and the ALP luminosities are always lower than the neutrino luminosity in our simulations. We estimate the number of neutrino events for Super-Kamiokande assuming a 10 kpc CCSN. We conclude that signatures of ALPs could be found in the long-term neutrino signals from a nearby CCSN event in the future, even if $g_{a\gamma}$ is below an upper limit based on the conventional energy-loss argument.

I. INTRODUCTION

Axion-like particles (ALPs) are a type of the beyond-standard-model particle and pseudo-Nambu-Goldstone bosons predicted by some string theories [1, 2]. ALPs could interact with photons through the coupling term below [3]:

$$\mathcal{L} = -\frac{1}{4}g_{a\gamma}F_{\mu\nu}\tilde{F}^{\mu\nu}a, \quad (1)$$

where a is the ALP field, $g_{a\gamma}$ is the coupling constant, $F_{\mu\nu}$ is the electromagnetic tensor and $\tilde{F}^{\mu\nu}$ is its dual.

Axion was first introduced to solve the strong CP problem and is a candidate of dark matter. It has been searched for with various methods including collider experiments [4–6], which have excluded $g_{a\gamma} \gtrsim 10^{-7} \text{ GeV}^{-1}$. Astronomical observations and cosmological arguments including Big Bang nucleosynthesis and the cosmic microwave background have also provided constraints on the ALP parameters [7, 8].

Astrophysical objects such as stars and supernovae can produce ALPs. Comparison of theoretical models including these effects and astronomical observation provides various constraints on ALP parameters. For instance, ALPs enhance energy loss in stars and affect the late phase of stellar evolution of stars with initial masses less than $8M_{\odot}$, stellar populations, and the structure of asymptotic giant branch stars [9, 34, 35]. The energy loss leads to a different initial-final mass relation of white dwarfs [10].

Among astrophysical objects, core-collapse supernovae (CCSNe) could be prolific sources of ALPs. ALPs formed in the supernova core extract energy from the star, thereby accelerating its cooling as a result. In addition, ALPs can assist collapsing stars in exploding if ALPs decay in the gain region and deposit heat into the surrounding matter. From the observation of SN 1987A, which is humanity's only detection of neutrinos from a CCSN so far and the first example of the multi-messenger astronomy, the ALP parameters have been constrained [11–14]. Moreover, heavy ALPs decay into gamma rays while traveling to the earth. The fact that no gamma ray has been detected provides a constraint [15] and the coupling constant between approximately $10^{-10} - 10^{-9} \text{ GeV}^{-1}$ has been excluded. In 2023, SN 2023ixf occurred at 6.9 Mpc, relatively near the earth. A Fermi-LAT observation of γ -rays from this object provided another constraint [16]. In the future, photons from nearby supernovae including type Ia supernovae and hypernovae may provide additional constraints [17–20].

In the context of simulations of ALP emission from CCSNe, there are two kinds of simulations: post-process simulations and self-consistent simulations with the ALP feedback. Although in both simulations ALP production is investigated [12, 21–24], we need self-consistent simulations for discussion on modification of neutrino emissions and hydrodynamics [25–27]. Table I summarizes previous self-consistent simulations. The previous works [25, 26, 28] considered axion-nucleon coupling for milli-electron-volt (meV) scale ALPs. On the other hand, Refs. [23, 29, 30] conducted simulations with axion-photon couplings of mega-electron-volt (MeV) scale ALPs. We note that there are simulations that solve not hydrodynamics but the hydrostatic equilibrium of proto-neutron stars to calculate the neutrino and axion emission [31, 32].

In this study, we focus on MeV scale ALPs, which

* Also at National Astronomical Observatory of Japan; masamitsu.mori.astro@gmail.com; masamitsu.mori@numazu-ct.ac.jp

we refer to as heavy ALPs. In Refs. [25, 26, 28], they estimated neutrino signals modified by ALPs. In Ref. [29], 2D simulations have been conducted and multi-messenger signals including gravitational waves have been estimated. The studies [23, 30] have discussed in the explodability of CCSNe. In this paper, we conduct long-term self-consistent 1D simulations with axion-photon coupling with 10 MeV ALPs and make a discussion on modification and observation of neutrinos.

In this paper, Section II describes the method of our calculation and Section III shows the calculation results: fluid, neutrino and ALP properties. In Section IV, we discuss neutrino events and a possibility to find ALPs or constraint on ALP parameters via a Galactic CCSN.

II. METHOD

A. CCSN simulation

We employ GR1D as a CCSN simulator. GR1D is an open-source general relativistic fluid simulator with neutrino radiation transport in one dimension [36, 37]. GR1D is implemented with the truncated moment scheme (M1 scheme) [38, 39] for neutrino transport. We modify the original version of GR1D for long-term simulation and axion cooling. The settings of the CCSN simulation without the ALP and the modifications for the long-term simulation are described in Ref. [40].

In this study, axion cooling is implemented in GR1D. The ALP production is calculated at every time step according to density, temperature and electron fraction of matter at that time. The heat taken away by ALPs is treated as feedback to the internal energy in the next time step. It is assumed that the ALP escapes from proto-neutron stars before they decay and proto-neutron stars cool down in the aftermath of the escape of ALPs. We use a $9.6M_{\odot}$ progenitor (provided by A. Heger 2016 private communication), which is reported to explode in 1D [40–42], and to form $1.36M_{\odot}$ after the explosion. The DD2 equation of state (EoS) [43–45] is employed as an EoS table, which is based on the density-dependent mean field theory.

B. Axion-Like Particle (ALP)

In this study, we consider two channels of ALP production: the photon coalescence and the Primakoff effect. Our treatment for the ALP production processes follows Refs. [12, 23, 29]. We fix the mass of ALPs to 10 MeV and choose $1 \times 10^{-9} \text{ GeV}^{-1}$ to $7 \times 10^{-9} \text{ GeV}^{-1}$ as the coupling constants $g_{a\gamma}$, because such ALPs evade constraints from the Sun [33?]. In Ref. [12], the same processes are calculated in post process and then the coupling constants above or equal to $6 \times 10^{-9} \text{ GeV}^{-1}$ are excluded via neutrinos of SN 1987A. It should be noted that we do not

consider ALP heating because 10 MeV ALPs are not expected to heat the gain region in the stellar cores [23]. Thus we ignore ALP decay and its heating.

In our calculation, we turn the axion processes on from the beginning of core collapse for two simulations with $g_{a\gamma} = 7.0 \times 10^{-9} \text{ GeV}^{-1}$ and $6.0 \times 10^{-9} \text{ GeV}^{-1}$. For smaller coupling constants, we begin calculating the ALP cooling after the shock wave escapes from the calculation region in order to save computational resources. We compare shock wave propagation for simulations with $g_{a\gamma} = 7.0 \times 10^{-9} \text{ GeV}^{-1}$ and $6.0 \times 10^{-9} \text{ GeV}^{-1}$ with that without ALP.

For convenience, we define a dimensionless constant g_{10} :

$$g_{10} = g_{a\gamma} \times 10^{10} \text{ GeV}. \quad (2)$$

Hereafter we employ g_{10} instead of $g_{a\gamma}$.

III. RESULTS

A. Shock wave propagation

Figure 1 shows radii of shock waves of the simulation without ALP (the reference model) and the simulations with $g_{10} = 70$ and 60 , which are the largest coupling constants in our simulations. Figure 1 indicates that the three curves completely overlap and the ALP cooling does not affect fluid dynamics and explodability in our simulations at all. It also agrees with the result in a previous work [23]. Thus, we turn the ALP cooling on after the shock wave escapes from the calculation region in order to save computational costs.

B. Temperature profiles

Figure 2 shows temperature versus density plots at 1 s, 5 s, 10 s, and 20 s after the bounce. Hereafter, we use the following color scheme: orange corresponds to 60, green to 50, red to 40, purple to 30, brown to 20, pink to 10, and grey represents the no ALP case (the reference model). At 1 s after the bounce, there is little difference among the simulations. By 5 s, the temperature declines above $10^{13} \text{ g cm}^{-3}$. At 10 s, the differences continue to grow and expand down to 10^8 g cm^{-3} . At last by 20 s, the outer layers have cooled due to the presence of ALPs. The hierarchy of the temperature profiles follows the order of the coupling constants $g_{a\gamma}$. These results show that PNS cooling is enhanced by ALP emission, particularly in the late phase.

C. ALP emission

Figure 3 shows the comparison of ALP luminosities. The right panel shows emissions via the photon coalescence and the left panel shows those from the Primakoff

TABLE I. Summary of supernova simulations including ALPs.

Authors	Year	Progenitor mass[M_{\odot}]	Gravity	Neutrino	Axion mass	Axion interacting matter	Dimension	Length [s]
M. Mori & K. Mori (This work)	2025	9.6	G.R.	M1	10 MeV	Photon	1D	20
T. Fischer et al. [25]	2016	18, 11.2	G.R.	Boltzmann	30 meV	Nucleon	1D	40
T. Fischer et al. [26]	2021	18	G.R.	Boltzmann	15 meV	Nucleon, Pion	1D	10
A. Betranhandy et al. [28]	2022	18	Effective	M1	11-114 meV	Nucleon	1D	4.5
		20			57-114 meV		2D	0.8
K. Mori et al. [23]	2023	20	Effective	IDSA	50-800 MeV	Photon	1D	0.5
		11.2			100 MeV			
K. Mori et al. [29]	2024	20	Effective	IDSA	100,200 MeV	Photon	2D	0.4
T. Tsurugi et al. [30]	2025	11.2,20,25	Effective	IDSA	50-800 MeV	Photon	1D	0.5

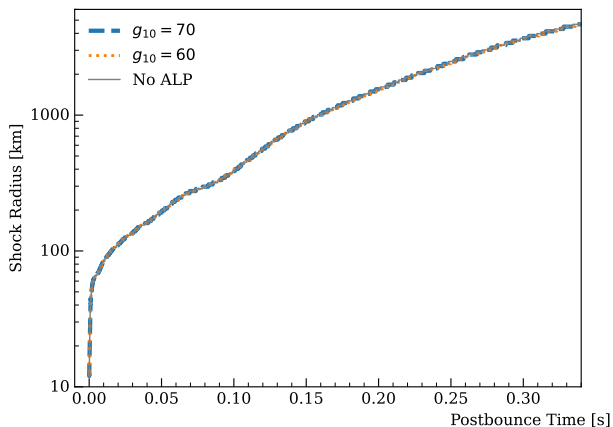


FIG. 1. Radius of shock wave with time. There are three curves and they completely overlap.

effect and neutrino luminosity including all flavors as the reference. The luminosities via the photon coalescence are from 10^{49} erg/s to 10^{47} erg/s at the bounce and they decrease to between about 10^{43} erg/s to 10^{44} erg/s. The hierarchy follows the order of the coupling constants and is kept until 20 s. We attribute the kink around 7.5 s in the curve of the $g_{10} = 70$ model to insufficient resolution, which results from the strong cooling rate and rapid contraction. The luminosities via the Primakoff effect increase more slowly and reach peaks after 1 s. The order of peak heights also corresponds to the order of the coupling constants. Then, the luminosities gradually decay. After 5 s in post-bounce time, the luminosities begin to cross each other. The decay rate of luminosity of the model with $g_{10} = 70$ is the highest and the second lowest luminosity at 20 s after the bounce. The third lowest luminosity corresponds to $g_{10} = 60$ and has the second highest peak at 2 s. However, the model with $g_{10} = 10$ always maintains the lowest luminosity. Comparing to the neutrino luminosity, the luminosities with $g_{10} = 70$ and $g_{10} = 60$ exceed the neutrino luminosity between 1.5 s to 4.0 s, which is consistent with the result in Ref. [9]. They obtained a constraint of $g_{10} \gtrsim 60$ based

on the criterion that ALP luminosities must not exceed the total neutrino luminosity at 1 s after the bounce. By contrast, the other ALP luminosities invariably are lower than that of neutrino.

Comparing the two panels proves that the Primakoff effect is considerably dominant. The ALP luminosities via the Primakoff effect is four to six orders of magnitude higher than those via the photon coalescence. Thus, the Primakoff effect determines luminosities in our simulations.

D. Neutrino emission

Figure 4 shows comparison of neutrino luminosities of electron neutrino ν_e , anti-electron neutrino $\bar{\nu}_e$ and heavy-lepton neutrino ν_x . We compare luminosities of each neutrino flavor across models. For all of the three flavors, the luminosities take their peaks at the bounce and monotonically decrease. The luminosities decrease more largely for the larger coupling constants in the late phase. Comparing the model with $g_{10} = 70$ to the no ALP model, the former luminosities are about one-tenth smaller than those of the latter for all flavors. The luminosities of the model with $g_{10} = 10$ are almost the same as those of the reference model.

Figure 5 shows the time evolution of average energies of neutrinos. Our definition of the average energy is

$$\langle E_{\nu} \rangle = \frac{\int E f(E) dE}{\int f(E) dE}, \quad (3)$$

with $f(E)$ the spectrum energy density. The tendency of influence of ALPs is the same as that in luminosities. The larger coupling constant ALPs more largely decrease neutrino average energies. The average energies of the model with $g_{a\gamma} = 7.0 \times 10^{-9} \text{ GeV}^{-1}$ are lower by 3 MeV than those of the reference model. In contract, the difference between average energies of the model with $g_{a\gamma} = 1.0 \times 10^{-9} \text{ GeV}^{-1}$ and those of the reference model are about 0.1 MeV at 20 s.

Figure 6 shows the number spectra at 1 s, 10 s and 20 s after the bounce for three flavors and each model. At 1 s, all the spectra are overlapped. At 10 s, the energy spectra begin to decrease and the differences become more

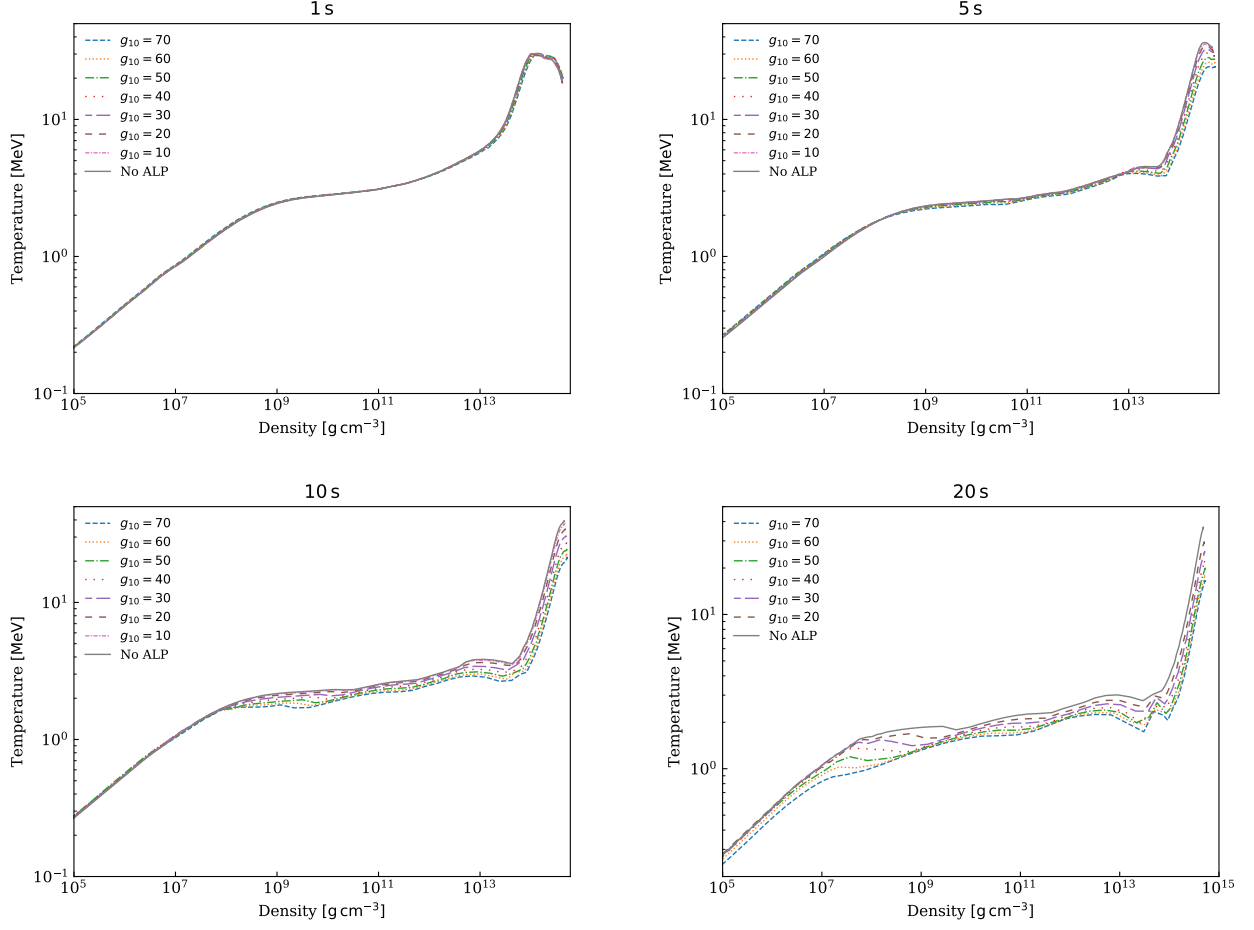


FIG. 2. Temperature versus density. The upper-left plot corresponds to curves at 1 s after the bounce: the upper-right plot corresponds to 5 s, the lower-left plot to 10 s and the lower-right plot to at 20 s. Regarding the color assignment: the blue corresponds to $g_{a\gamma} = 70 \text{ GeV}^{-1}$, the orange to 60, the green to 50, the red to 40, the purple to 30, the brown to 20, the pink to 10 and the gray to the no ALP case.

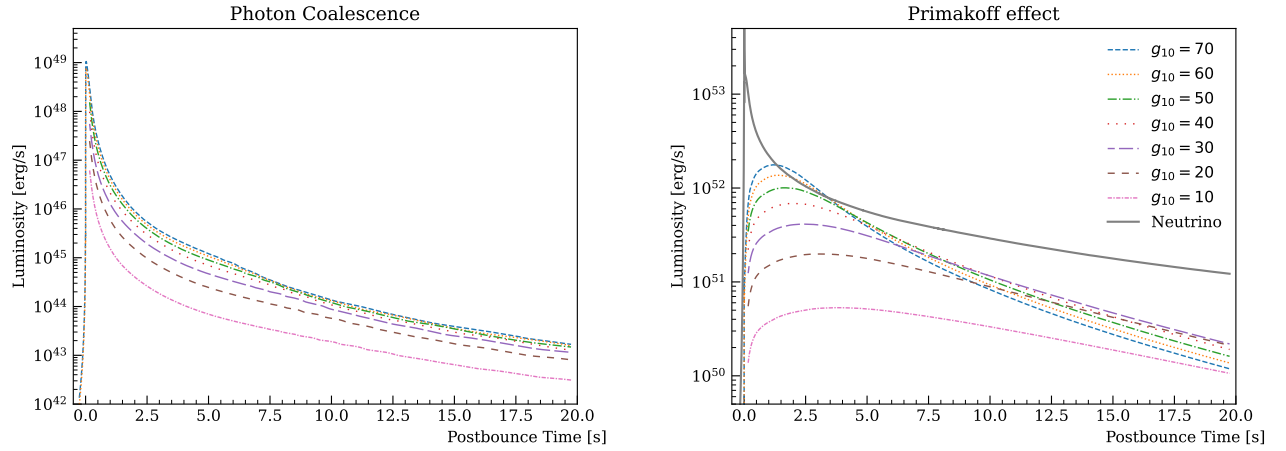


FIG. 3. ALP luminosities. The left panel represents that via the photon coalescence and the right panel represents that via the Primakoff effect and the total neutrino luminosity of the reference model. The color assignment follows Figure 2.

pronounced, especially at higher energies. The energy hierarchy is kept for all flavors until 20 s. Figures 4, 5 and 6 show neutrinos reflect the cooling enhanced by the ALPs.

We show the dependence of cumulative energy emitted via neutrinos and ALPs on the coupling constants g_{10} in Figure 7. The emitted energy of neutrinos up to 1.0 s is 5.5×10^{52} erg and invariable for g_{10} . At 10 s and 20 s the cumulative energy emitted as neutrinos decreases from 1.24×10^{52} erg and 1.40×10^{52} erg to 1.23×10^{52} erg and 1.25×10^{52} erg for as the total energy emitted ALPs increases to 6.2×10^{52} erg.

IV. DISCUSSION

This section describes the discussion on neutrino observation and the possibility to find ALP signals from neutrino events. Here we assume Super-Kamiokande as a neutrino detector.

A. Neutrino detection

Supernova neutrinos can be detected via underground detectors. The Super-Kamiokande (SK) detector [46] is a large water-Cherenkov detector in Japan. The SK detector is monitoring supernovae for 24 hours and issues alert to observatories all over the world if it detects supernovae [47]. SK observes mainly supernova neutrinos via the inverse beta decay (IBD) [48],

$$\bar{\nu}_e + p^+ \rightarrow n + e^+. \quad (4)$$

in which a proton p and an electron antineutrino $\bar{\nu}_e$ interact and produce a neutron n and a positron e^+ . SK has 100 % sensitivity for galactic supernovae [49, 50]. SK employs the full of 32.5 kton of water in the inner detector and some thousands of neutrinos can interact in the SK detector [50]. We assume that CCSNe occur at 10 kpc away from the Earth, neutrino flavors mix following the MSW oscillation [51, 52] during traveling, mass hierarchy is normal, and neutrinos interact only via the IBD in the SK detector.

Figure 8 shows the event rates and the cumulative event numbers. The event rate and also the cumulative events almost overlap until 1 s after the bounce. After 2 s after the bounce, the curves start to separate from each other. At 20 s after the bounce, the event rate of the model with $g_{10} = 70$ decreases below 1 Hz and smaller than 5 % of that of the reference model. This discrepancy arises because event rates depend on both the luminosity and the average energy of neutrinos.

The right panel in Figure 8 shows cumulative events. The time evolutions of cumulative events also overlap until 1 s after the bounce and the time evolutions begin to separate from each other. Even after 10 s, the cumulative events continue to increase. The number of cumulative

events of the reference model reaches 1,750 events at 20 s and on the other hand, that of the model with $g_{10} = 70$ reaches 1,250 events.

Figure 9 plots the numbers of cumulative events at 1 s, 10 s and 20 s after the bounce with error bars. We assume the Poisson distribution and the definition of error bars writes $\sqrt{N(t)}$ with $N(t)$ the number of cumulative events at t . We put the errors upward and downward around the center values. At 1 s after the bounce, we cannot discriminate the models. However, we might discriminate the model with the coupling constants above $g_{10} = 30$, which might expand constraint on the ALP parameters.

B. Future plan

Next, we will conduct simulations of various progenitors. There are a few red supergiants that may be close to undergoing a CCSN such as Betelgeuse. We plan to simulate specific red supergiant progenitors located near Earth [53, 54] and in the local galaxies [55].

Supernovae can result in black holes instead of neutron stars [56–58]. Simulating core collapse leading to black hole formation is more challenging, as it requires fully incorporating general relativity, and involves higher densities and temperatures. These extreme conditions can produce more ALPs than those produced in the neutron star-forming case. This makes such simulations a worthwhile next step.

In the future, we will construct an analytic formula of neutrino luminosity and event rate and develop a method for estimating existence of ALPs. Analytical late-phase neutrino luminosity and event rate models have been developed in Ref. [59] and the methods for estimating PNS mass, radius and so on from neutrinos using the analytic formula have also been proposed [60–62]. Then, an analytic ALP luminosity has been derived [63]. We will incorporate the effect of ALPs as the additional generation of leptons into the formulae in Ref. [59]. The modification effectively model the cooling effect of ALPs.

V. SUMMARY

In this paper, we described the long-term simulations with the general relativistic neutrino radiation hydrodynamics including axion cooling, in which ALP mass is 10 MeV and coupling constants are from $10 \times 10^{-9} \text{ GeV}^{-1}$ to $70 \times 10^{-9} \text{ GeV}^{-1}$ and investigated influences of ALPs on fluid and neutrino emission. The ALPs accelerate the PNS cooling. We found that the effects of ALPs do not emerge in the early phase until 1 s after the bounce but in the late phase on our zero-metallicity $9.6 M_\odot$ progenitor. We assumed that supernovae occur at 10 kpc away and are observed with SK. The event rate and cumulative events significantly decrease in the late phase. If we detect neutrinos from Galactic supernovae, we might find

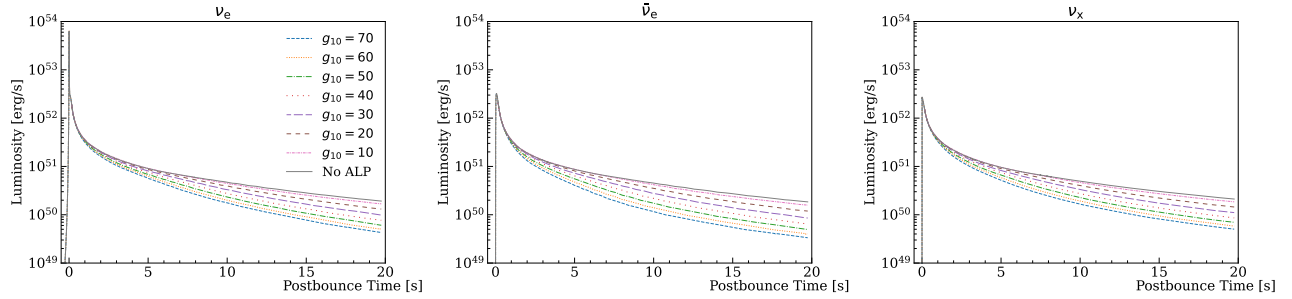


FIG. 4. Neutrino luminosities. The left panel is luminosities of electron neutrino ν_e and the middle panel is those of anti-electron neutrino $\bar{\nu}_e$ and the right panel is those of heavy-lepton neutrino ν_χ . The color assignment follows Figure 2.

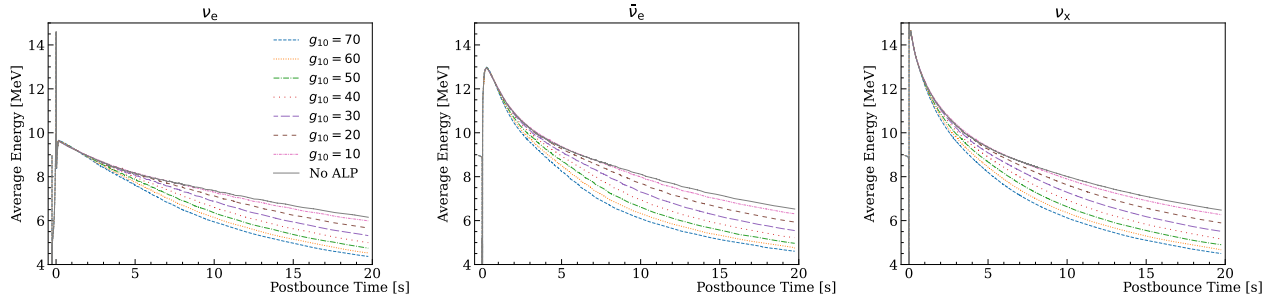


FIG. 5. Neutrino average energies. The left panel is average energies of electron neutrino ν_e and the middle panel is those of anti-electron neutrino $\bar{\nu}_e$ and the right panel is those of heavy-lepton neutrino ν_χ .

an indication of an ALP that evade the constraint based on the conventional energy-loss argument.

ACKNOWLEDGMENTS

We thank Yudai Suwa, Tomoya Takiwaki, Kohsuke Sumiyoshi and the all members of the nuLC collabora-

tion [64] for discussions. This work is supported by JSPS KAKENHI Grant Numbers JP23KJ2147, JP23K13107, JP23KJ2150, and JP25H02194.

-
- [1] L. Di Luzio, M. Giannotti, E. Nardi, and L. Visinelli, Corrigendum to “The landscape of QCD axion models” [Phys. Rep. 870 (2020) 1-117], Physics Reports **870**, 1 (2020), arXiv:2003.01100 [hep-ph].
 - [2] K. Choi, S. H. Im, and C. S. Shin, Recent Progress in the Physics of Axions and Axion-Like Particles, Annual Review of Nuclear and Particle Science **71**, 225 (2021), arXiv:2012.05029 [hep-ph].
 - [3] G. Raffelt and L. Stodolsky, Mixing of the photon with low-mass particles, Phys. Rev. D **37**, 1237 (1988).
 - [4] J. Jaeckel and M. Spannowsky, Probing MeV to 90 GeV axion-like particles with LEP and LHC, Physics Letters B **753**, 482 (2016), arXiv:1509.00476 [hep-ph].
 - [5] B. Döbrich, J. Jaeckel, and T. Spadaro, Light in the beam dump. Axion-Like Particle production from decay photons in proton beam-dumps, Journal of High Energy Physics **2019**, 213 (2019).
 - [6] M. J. Dolan, T. Ferber, C. Hearty, F. Kahlhoefer, and K. Schmidt-Hoberg, Revised constraints and Belle II sensitivity for visible and invisible axion-like particles, Journal of High Energy Physics **2017**, 94 (2017), arXiv:1709.00009 [hep-ph].
 - [7] D. Cadamuro and J. Redondo, Cosmological bounds on pseudo Nambu-Goldstone bosons, Journal of Cosmology and Astroparticle Physics **2012** (2), 032, arXiv:1110.2895 [hep-ph].
 - [8] P. F. Depta, M. Hufnagel, and K. Schmidt-Hoberg, Robust cosmological constraints on axion-like particles, Journal of Cosmology and Astroparticle Physics **2020** (5), 009, arXiv:2002.08370 [hep-ph].
 - [9] P. Carenza, O. Straniero, B. Döbrich, M. Giannotti, G. Lucente, and A. Mirizzi, Constraints on the coupling with photons of heavy axion-like-particles from Globular Clusters, Physics Letters B **809**, 135709 (2020), arXiv:2004.08399 [hep-ph].

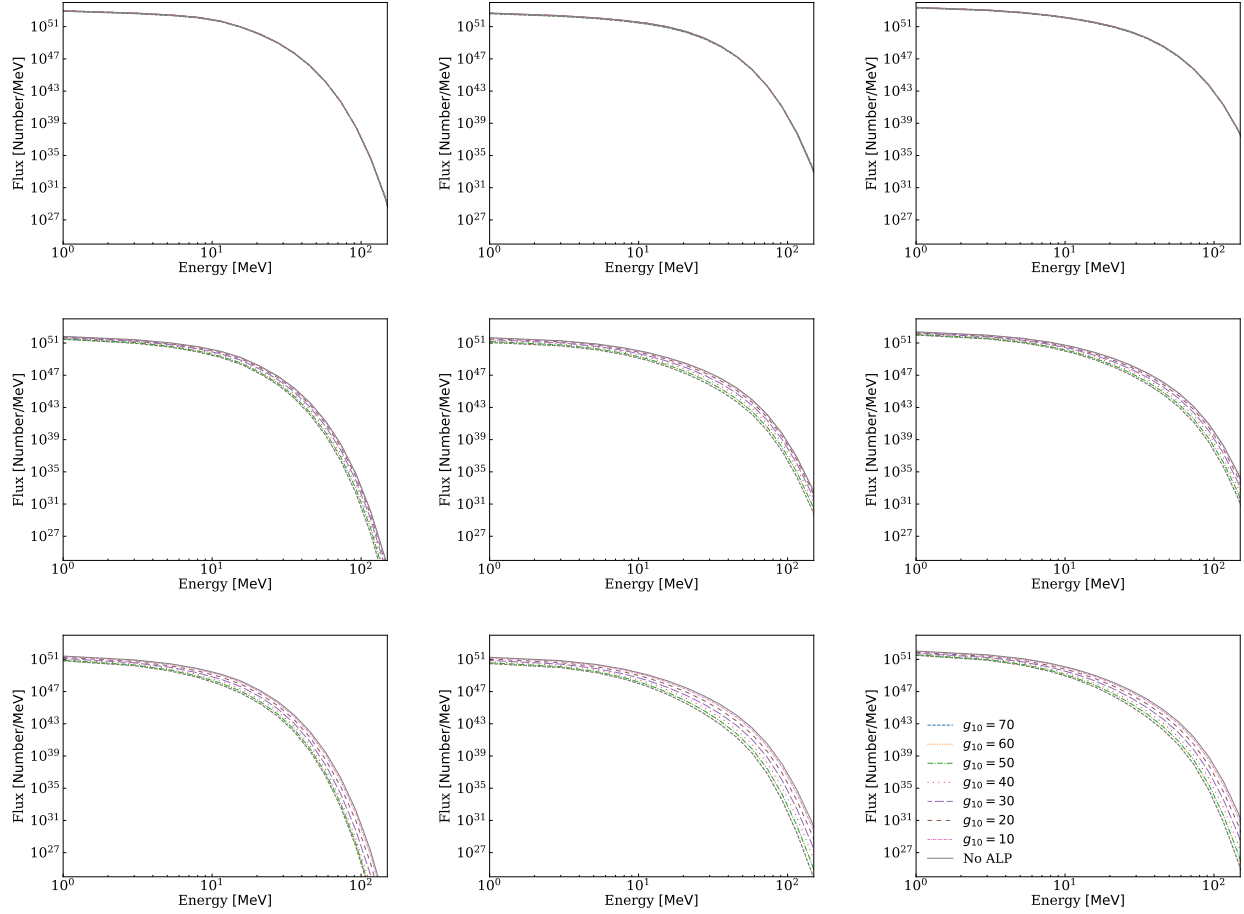


FIG. 6. Neutrino number spectra. The horizontal axis is neutrino energy in MeV and the vertical axis is number flux per MeV. The panels are arranged vertically in time and horizontally in flavors. The left column is 1 s after the bounce, the middle column is 10 s after the bounce and the right column is 20 s after the bounce. The top row is ν_e , the middle row is $\bar{\nu}_e$ and the bottom row is ν_χ .

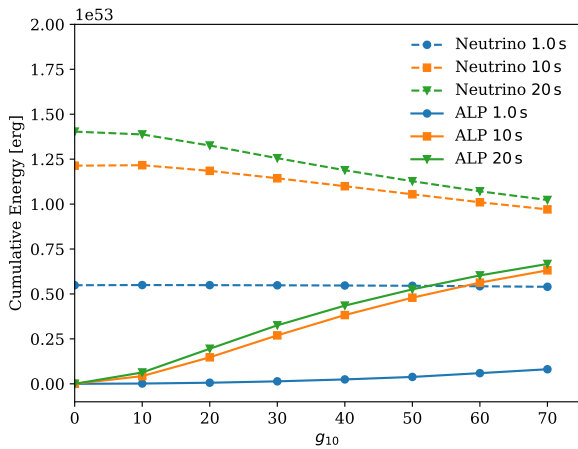


FIG. 7. Cumulative energy emitted via neutrinos and ALPs versus coupling constants g_{10} . The solid curves mean neutrino and the dashed curves mean ALP. The blue corresponds to 1.0 s, the orange to 10 s and the green to 20 s after the bounce.

- [10] M. J. Dolan, F. J. Hiskens, and R. R. Volkas, Constraining axion-like particles using the white dwarf initial-final mass relation, *Journal of Cosmology and Astroparticle Physics* **2021** (9), 010, arXiv:2102.00379 [hep-ph].
- [11] J. S. Lee, Revisiting Supernova 1987A Limits on Axion-Like-Particles, arXiv e-prints, arXiv:1808.10136 (2018), arXiv:1808.10136 [hep-ph].
- [12] G. Lucente, P. Carenza, T. Fischer, M. Giannotti, and A. Mirizzi, Heavy axion-like particles and core-collapse supernovae: constraints and impact on the explosion mechanism, *Journal of Cosmology and Astroparticle Physics* **2020** (12), 008, arXiv:2008.04918 [hep-ph].
- [13] A. Sung, H. Tu, and M.-R. Wu, New constraint from supernova explosions on light particles beyond the Standard Model, *Phys. Rev. D* **99**, 121305 (2019), arXiv:1903.07923 [hep-ph].
- [14] A. Caputo, H.-T. Janka, G. Raffelt, and E. Vitagliano, Low-Energy Supernovae Severely Constrain Radiative Particle Decays, *Phys. Rev. Lett.* **128**, 221103 (2022), arXiv:2201.09890 [astro-ph.HE].
- [15] S. Hoof and L. Schulz, Updated constraints on axion-like particles from temporal information in supernova

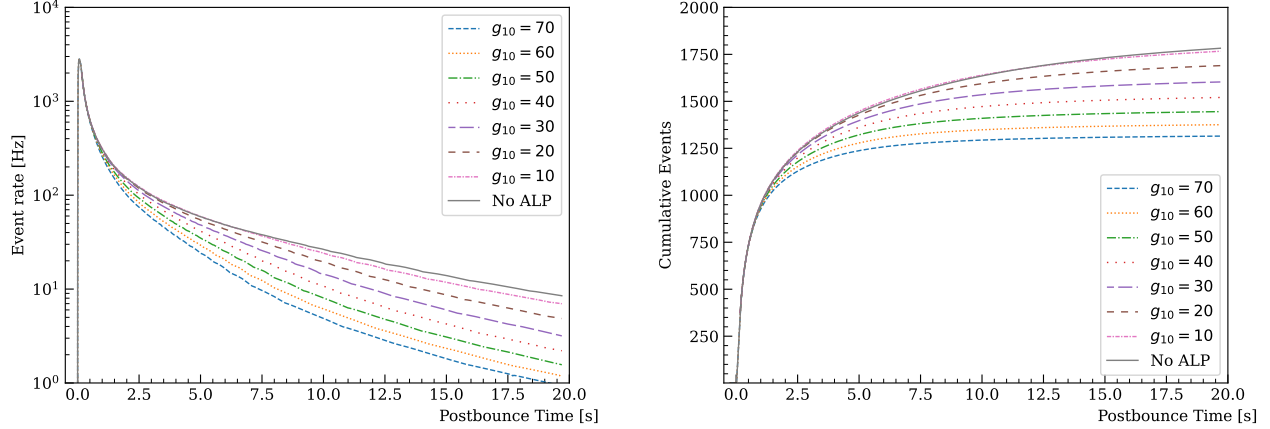


FIG. 8. Neutrino event rate (left) and the cumulative number of events (right). It is assumed that CCSNe occurs at 10 kpc away.

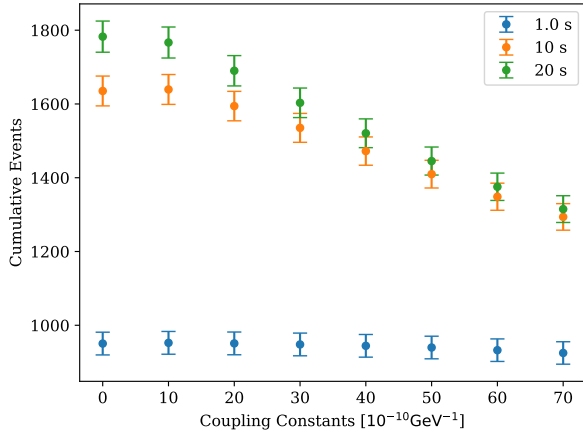


FIG. 9. Comparison of the number of cumulative events versus the coupling constants at 1s, 10s and 20s after the bounce. The error bars indicate errors of the Poisson distribution.

- SN1987A gamma-ray data, *Journal of Cosmology and Astroparticle Physics* **2023** (3), 054, arXiv:2212.09764 [hep-ph].
- [16] E. Ravensburg, P. Carenza, C. Eckner, and A. Goobar, Constraining MeV-scale axionlike particles with Fermi-LAT observations of SN 2023ixf, *Phys. Rev. D* **109**, 023018 (2024), arXiv:2306.16397 [astro-ph.HE].
- [17] M. Giannotti, L. D. Duffy, and R. Nita, New constraints for heavy axion-like particles from supernovae, *Journal of Cosmology and Astroparticle Physics* **2011** (1), 015, arXiv:1009.5714 [astro-ph.HE].
- [18] J. Jaeckel, P. C. Malta, and J. Redondo, Decay photons from the axionlike particles burst of type II supernovae, *Phys. Rev. D* **98**, 055032 (2018), arXiv:1702.02964 [hep-ph].
- [19] K. Mori, Heavy axion-like particles and MeV decay photons from nearby type Ia supernovae, *Publications of the Astronomical Society of Japan* **73**, 1382 (2021), arXiv:2107.09097 [hep-ph].
- [20] A. Caputo, P. Carenza, G. Lucente, E. Vitagliano, M. Giannotti, K. Kotake, T. Kuroda, and A. Mirizzi, Axionlike Particles from Hypernovae, *Phys. Rev. Lett.* **127**, 181102 (2021), arXiv:2104.05727 [hep-ph].
- [21] A. Caputo, G. Raffelt, and E. Vitagliano, Muonic boson limits: Supernova redux, *Phys. Rev. D* **105**, 035022 (2022), arXiv:2109.03244 [hep-ph].
- [22] E. Müller, F. Calore, P. Carenza, C. Eckner, and M. C. D. Marsh, Investigating the gamma-ray burst from decaying MeV-scale axion-like particles produced in supernova explosions, *Journal of Cosmology and Astroparticle Physics* **2023** (7), 056, arXiv:2304.01060 [astro-ph.HE].
- [23] P. Carenza, Axion emission from supernovae: a cheat-sheet, *European Physical Journal Plus* **138**, 836 (2023), arXiv:2309.14798 [hep-ph].
- [24] P. Carenza, T. Fischer, M. Giannotti, G. Guo, G. Martínez-Pinedo, and A. Mirizzi, Improved axion emissivity from a supernova via nucleon-nucleon bremsstrahlung, *Journal of Cosmology and Astroparticle Physics* **2019** (10), 016, arXiv:1906.11844 [hep-ph].
- [25] T. Fischer, S. Chakraborty, M. Giannotti, A. Mirizzi, A. Payez, and A. Ringwald, Probing axions with the neutrino signal from the next Galactic supernova, *Phys. Rev. D* **94**, 085012 (2016), arXiv:1605.08780 [astro-ph.HE].
- [26] T. Fischer, P. Carenza, B. Fore, M. Giannotti, A. Mirizzi, and S. Reddy, Observable signatures of enhanced axion emission from protoneutron stars, *Phys. Rev. D* **104**, 103012 (2021), arXiv:2108.13726 [hep-ph].
- [27] K. Mori, T. Takiwaki, K. Kotake, and S. Horiuchi, Shock revival in core-collapse supernovae assisted by heavy axionlike particles, *Phys. Rev. D* **105**, 063009 (2022), arXiv:2112.03613 [astro-ph.HE].
- [28] A. Betranhandy and E. O'Connor, Neutrino driven explosions aided by axion cooling in multidimensional simulations of core-collapse supernovae, *Phys. Rev. D* **106**, 063019 (2022), arXiv:2204.00503 [astro-ph.HE].

- [29] K. Mori, T. Takiwaki, K. Kotake, and S. Horiuchi, Two-dimensional models of core-collapse supernova explosions assisted by heavy sterile neutrinos, *Phys. Rev. D* **110**, 023031 (2024), arXiv:2402.14333 [astro-ph.HE].
- [30] T. Takata, K. Mori, K. Nakamura, and K. Kotake, Progenitor Dependence of Neutrino-driven Supernova Explosions with the Aid of Heavy Axion-like Particles, arXiv e-prints, arXiv:2503.09005 (2025), arXiv:2503.09005 [astro-ph.HE].
- [31] A. Burrows, M. S. Turner, and R. P. Brinkmann, Axions and SN 1987A, *Phys. Rev. D* **39**, 1020 (1989).
- [32] W. Keil, H.-T. Janka, D. N. Schramm, G. Sigl, M. S. Turner, and J. Ellis, Fresh look at axions and SN 1987A, *Phys. Rev. D* **56**, 2419 (1997), arXiv:astro-ph/9612222 [astro-ph].
- [33] N. Vinyoles, A. Serenelli, F. L. Villante, S. Basu, J. Redondo, and J. Isern, New axion and hidden photon constraints from a solar data global fit, *Journal of Cosmology and Astroparticle Physics* **2015** (10), 015, arXiv:1501.01639 [astro-ph.SR].
- [34] A. Ayala, I. Domínguez, M. Giannotti, A. Mirizzi, and O. Straniero, Revisiting the Bound on Axion-Photon Coupling from Globular Clusters, *Phys. Rev. Lett.* **113**, 191302 (2014), arXiv:1406.6053 [astro-ph.SR].
- [35] M. J. Dolan, F. J. Hiskens, and R. R. Volkas, Advancing globular cluster constraints on the axion-photon coupling, *JCAP* **10**, 096, arXiv:2207.03102 [hep-ph].
- [36] E. O'Connor and C. D. Ott, A new open-source code for spherically symmetric stellar collapse to neutron stars and black holes, *Classical and Quantum Gravity* **27**, 114103 (2010), arXiv:0912.2393 [astro-ph.HE].
- [37] E. O'Connor, An Open-source Neutrino Radiation Hydrodynamics Code for Core-collapse Supernovae, *The Astrophysical Journal Supplement Series* **219**, 24 (2015), arXiv:1411.7058 [astro-ph.HE].
- [38] M. Shibata, K. Kiuchi, Y. Sekiguchi, and Y. Suwa, Truncated Moment Formalism for Radiation Hydrodynamics in Numerical Relativity, *Progress of Theoretical Physics* **125**, 1255 (2011), arXiv:1104.3937 [astro-ph.HE].
- [39] C. Y. Cardall, E. Endeve, and A. Mezzacappa, Conservative 3+1 general relativistic variable Eddington tensor radiation transport equations, *Phys. Rev. D* **87**, 103004 (2013), arXiv:1209.2151 [astro-ph.HE].
- [40] M. Mori, Y. Suwa, K. Nakazato, K. Sumiyoshi, M. Harada, A. Harada, Y. Koshio, and R. A. Wendell, Developing an end-to-end simulation framework of supernova neutrino detection, *Progress of Theoretical and Experimental Physics* **2021**, 023E01 (2021), arXiv:2010.16254 [astro-ph.HE].
- [41] T. Melson, H.-T. Janka, and A. Marek, Neutrino-driven Supernova of a Low-mass Iron-core Progenitor Boosted by Three-dimensional Turbulent Convection, *The Astrophysical Journal* **801**, L24 (2015), arXiv:1501.01961 [astro-ph.SR].
- [42] D. Radice, A. Burrows, D. Vartanyan, M. A. Skinner, and J. C. Dolence, Electron-capture and Low-mass Iron-core-collapse Supernovae: New Neutrino-radiation-hydrodynamics Simulations, *Astrophys. J.* **850**, 43 (2017), arXiv:1702.03927 [astro-ph.HE].
- [43] S. Typel, Relativistic model for nuclear matter and atomic nuclei with momentum-dependent self-energies, *Phys. Rev. C* **71**, 064301 (2005), arXiv:nucl-th/0501056 [nucl-th].
- [44] M. Hempel and J. Schaffner-Bielich, A statistical model for a complete supernova equation of state, *Nuclear Physics A* **837**, 210 (2010), arXiv:0911.4073 [nucl-th].
- [45] S. Typel, G. Röpke, T. Klähn, D. Blaschke, and H. H. Wolter, Composition and thermodynamics of nuclear matter with light clusters, *Phys. Rev. C* **81**, 015803 (2010), arXiv:0908.2344 [nucl-th].
- [46] Y. Fukuda *et al.* (Super-Kamiokande), The Super-Kamiokande detector, *Nucl. Instrum. Meth. A* **501**, 418 (2003).
- [47] K. Abe, Y. Haga, Y. Hayato, M. Ikeda, K. Iyogi, J. Kameda, Y. Kishimoto, M. Miura, S. Moriyama, M. Nakahata, Y. Nakano, S. Nakayama, H. Sekiya, M. Shiozawa, Y. Suzuki, A. Takeda, H. Tanaka, T. Tomura, K. Ueno, R. A. Wendell, T. Yokozawa, T. Irvine, T. Kajita, I. Kametani, K. Kaneyuki, K. P. Lee, T. McLachlan, Y. Nishimura, E. Richard, K. Okumura, L. Labarga, P. Fernandez, S. Berkman, H. A. Tanaka, S. Tobayama, J. Gustafson, E. Kearns, J. L. Raaf, J. L. Stone, L. R. Sulak, M. Goldhaber, G. Carminati, W. R. Kropp, S. Mine, P. Weatherly, A. Renshaw, M. B. Smy, H. W. Sobel, V. Takhistov, K. S. Ganezer, B. L. Hartfiel, J. Hill, W. E. Keig, N. Hong, J. Y. Kim, I. T. Lim, T. Akiri, A. Himmel, K. Scholberg, C. W. Walter, T. Wongjirad, T. Ishizuka, S. Tasaka, J. S. Jang, J. G. Learned, S. Matsuno, S. N. Smith, T. Hasegawa, T. Ishida, T. Ishii, T. Kobayashi, T. Nakadaira, K. Nakamura, Y. Oyama, K. Sakashita, T. Sekiguchi, T. Tsukamoto, A. T. Suzuki, Y. Takeuchi, C. Bronner, S. Hirota, K. Huang, K. Ieki, T. Kikawa, A. Minamino, A. Murakami, T. Nakaya, K. Suzuki, S. Takahashi, K. Tateishi, Y. Fukuda, K. Choi, Y. Itow, G. Mitsuka, P. Mijakowski, J. Hignight, J. Imber, C. K. Jung, C. Yanagisawa, M. J. Wilking, H. Ishino, A. Kibayashi, Y. Koshio, T. Mori, M. Sakuda, R. Yamaguchi, T. Yano, Y. Kuno, R. Tacik, S. B. Kim, H. Okazawa, Y. Choi, K. Nishijima, M. Koshiha, Y. Suda, Y. Totsuka, M. Yokoyama, K. Martens, L. Marti, M. R. Vagins, J. F. Martin, P. de Perio, A. Konaka, S. Chen, Y. Zhang, K. Connolly, and R. J. Wilkes, Real-time supernova neutrino burst monitor at Super-Kamiokande, *Astroparticle Physics* **81**, 39 (2016), arXiv:1601.04778 [astro-ph.HE].
- [48] A. Strumia and F. Vissani, Precise quasielastic neutrino/nucleon cross-section, *Physics Letters B* **564**, 42 (2003), arXiv:astro-ph/0302055 [astro-ph].
- [49] M. Ikeda, A. Takeda, Y. Fukuda, M. R. Vagins, K. Abe, T. Iida, K. Ishihara, J. Kameda, Y. Koshio, A. Minamino, C. Mitsuda, M. Miura, S. Moriyama, M. Nakahata, Y. Obayashi, H. Ogawa, H. Sekiya, M. Shiozawa, Y. Suzuki, Y. Takeuchi, K. Ueshima, H. Watanabe, S. Yamada, I. Higuchi, C. Ishihara, M. Ishitsuka, T. Kajita, K. Kaneyuki, G. Mitsuka, S. Nakayama, H. Nishino, K. Okumura, C. Saji, Y. Takenaga, S. Clark, S. Desai, F. Dufour, E. Kearns, S. Likhoded, M. Litos, J. L. Raaf, J. L. Stone, L. R. Sulak, W. Wang, M. Goldhaber, D. Casper, J. P. Cravens, J. Dunmore, W. R. Kropp, D. W. Liu, S. Mine, C. Regis, M. B. Smy, H. W. Sobel, K. S. Ganezer, J. Hill, W. E. Keig, J. S. Jang, J. Y. Kim, I. T. Lim, K. Scholberg, N. Tanimoto, C. W. Walter, R. Wendell, R. W. Ellsworth, S. Tasaka, G. Guillian, J. G. Learned, S. Matsuno, M. D. Messier, Y. Hayato, A. K. Ichikawa, T. Ishida, T. Ishii, T. Iwashita, T. Kobayashi, T. Nakadaira, K. Nakamura, K. Nitta, Y. Oyama, Y. Totsuka, A. T. Suzuki,

- M. Hasegawa, K. Hiraide, H. Maesaka, T. Nakaya, K. Nishikawa, T. Sasaki, S. Yamamoto, M. Yokoyama, T. J. Haines, S. Dazeley, S. Hatakeyama, R. Svoboda, G. W. Sullivan, D. Turcan, A. Habig, T. Sato, Y. Itow, T. Koike, T. Tanaka, C. K. Jung, T. Kato, K. Kobayashi, M. Malek, C. McGrew, A. Sarra, R. Terri, C. Yanagisawa, N. Tamura, Y. Idehara, M. Sakuda, M. Sugihara, Y. Kuno, M. Yoshida, S. B. Kim, B. S. Yang, J. Yoo, T. Ishizuka, H. Okazawa, Y. Choi, H. K. Seo, Y. Gando, T. Hasegawa, K. Inoue, Y. Furuse, H. Ishii, K. Nishijima, H. Ishino, Y. Watanabe, M. Koshihara, S. Chen, Z. Deng, Y. Liu, D. Kielczewska, J. Zalipska, H. Berns, R. Gran, K. K. Shiraishi, A. Stachyra, E. Thrane, K. Washburn, R. J. Wilkes, and Super-KAMIOKANDE Collaboration, Search for Supernova Neutrino Bursts at Super-Kamiokande, *Astrophys. J.* **669**, 519 (2007), arXiv:0706.2283 [astro-ph].
- [50] M. Mori, K. Abe, Y. Hayato, K. Hiraide, K. Ieki, M. Ikeda, S. Imaizumi, J. Kameda, Y. Kanemura, R. Kaneshima, Y. Kashiwagi, Y. Kataoka, S. Miki, S. Mine, M. Miura, S. Moriyama, Y. Nagao, M. Nakahata, Y. Nakano, S. Nakayama, Y. Noguchi, T. Okada, K. Okamoto, A. Orii, K. Sato, H. Sekiya, H. Shiba, K. Shimizu, M. Shiozawa, Y. Sonoda, Y. Suzuki, A. Takeda, Y. Takemoto, A. Takenaka, H. Tanaka, T. Tomiya, S. Watanabe, T. Yano, S. Yoshida, S. Han, T. Kajita, K. Okumura, T. Tashiro, X. Wang, J. Xia, G. D. Megias, D. Bravo-Berguño, P. Fernandez, L. Labarga, N. Ospina, B. Zaldivar, S. Zsoldos, B. W. Pointon, F. D. M. Blaszczyk, E. Kearns, J. L. Raaf, J. L. Stone, L. Wan, T. Wester, J. Bian, N. J. Griskevich, W. R. Kropp, S. Locke, M. B. Smy, H. W. Sobel, V. Takhistov, A. Yankelevich, J. Hill, J. Y. Kim, I. T. Lim, R. G. Park, B. Bodur, K. Scholberg, C. W. Walter, L. Bernard, A. Coffani, O. Drapier, S. El Hedri, A. Giampaolo, T. A. Mueller, P. Paganini, B. Quilain, A. D. Santos, T. Ishizuka, T. Nakamura, J. S. Jang, J. G. Learned, L. H. V. Anthony, D. Martin, M. Scott, A. A. Sztuc, Y. Uchida, V. Berardi, M. G. Catanesi, E. Radicioni, N. F. Calabria, L. N. Machado, G. De Rosa, G. Collazuol, F. Iacob, M. Lamoureux, M. Mattiazzi, L. Ludovici, M. Gonin, G. Pronost, Y. Maekawa, Y. Nishimura, C. Fujisawa, M. Friend, T. Hasegawa, T. Ishida, T. Kobayashi, M. Jakkapu, T. Matsubara, T. Nakadaira, K. Nakamura, Y. Oyama, K. Sakashita, T. Sekiguchi, T. Tsukamoto, H. Ozaki, T. Shiozawa, A. T. Suzuki, Y. Takeuchi, S. Yamamoto, Y. Kotsar, Y. Ashida, C. Bronner, J. Feng, S. Hirota, T. Kikawa, T. Nakaya, R. A. Wendell, K. Yasutome, N. McCauley, P. Mehta, K. M. Tsui, Y. Fukuda, Y. Itow, H. Menjo, K. Ninomiya, T. Niwa, M. Tsukada, J. Lagoda, S. M. Lakshmi, P. Mijakowski, J. Zalipska, M. Mandal, Y. S. Prabhu, J. Jiang, C. K. Jung, C. Vilela, M. J. Wilking, C. Yanagisawa, M. Jia, K. Hagiwara, M. Harada, T. Horai, H. Ishino, S. Ito, H. Kitagawa, Y. Koshio, W. Ma, F. Nakanishi, N. Piplani, S. Sakai, G. Barr, D. Barrow, L. Cook, S. Samani, D. Wark, F. Nova, T. Boschi, J. Gao, A. Goldsack, T. Katori, F. Di Lodovico, J. Migenza, M. Taani, S. Zsoldos, J. Y. Yang, S. J. Jenkins, M. Malek, J. M. McElwee, O. Stone, M. D. Thiesse, L. F. Thompson, H. Okazawa, S. B. Kim, J. W. Seo, I. Yu, K. Nishijima, M. Koshihara, K. Nakagiri, Y. Nakajima, K. Iwamoto, N. Taniuchi, M. Yokoyama, K. Martens, and P. de Perio, Searching for Supernova Bursts in Super-Kamiokande IV, *Astrophys. J.* **938**, 35 (2022), arXiv:2206.01380 [astro-ph.HE].
- [51] A. S. Dighe and A. Y. Smirnov, Identifying the neutrino mass spectrum from a supernova neutrino burst, *Phys. Rev. D* **62**, 033007 (2000), arXiv:hep-ph/9907423 [hep-ph].
- [52] M.-R. Wu, Y.-Z. Qian, G. Martínez-Pinedo, T. Fischer, and L. Huther, Effects of neutrino oscillations on nucleosynthesis and neutrino signals for an 18 M_{\odot} supernova model, *Phys. Rev. D* **91**, 065016 (2015), arXiv:1412.8587 [astro-ph.HE].
- [53] M. Messineo and A. G. A. Brown, A Catalog of Known Galactic K-M Stars of Class I Candidate Red Supergiants in Gaia DR2, *The Astronomical Journal* **158**, 20 (2019), arXiv:1905.03744 [astro-ph.GA].
- [54] S. Healy, S. Horiuchi, M. Colomer Molla, D. Milisavljevic, J. Tseng, F. Bergin, K. Weil, M. Tanaka, and S. Otero, Red supergiant candidates for multimessenger monitoring of the next Galactic supernova, *Monthly Notices of the Royal Astronomical Society* **529**, 3630 (2024), arXiv:2307.08785 [astro-ph.SR].
- [55] Y. Ren, B. Jiang, M. Yang, T. Wang, and T. Ren, The Sample of Red Supergiants in 12 Low-mass Galaxies of the Local Group, *Astrophys. J.* **923**, 232 (2021), arXiv:2110.08793 [astro-ph.GA].
- [56] K. Sumiyoshi, H. Suzuki, and S. Yamada, Fate of core-collapse supernovae: formation of neutron star and black hole, in *Origin of Matter and Evolution of Galaxies*, American Institute of Physics Conference Series, Vol. 847, edited by S. Kubono, W. Aoki, T. Kajino, T. Motobayashi, and K. Nomoto (AIP, 2006) pp. 473–475.
- [57] K. Sumiyoshi, S. Yamada, and H. Suzuki, Dynamics and Neutrino Signal of Black Hole Formation in Nonrotating Failed Supernovae. I. Equation of State Dependence, *Astrophys. J.* **667**, 382 (2007), arXiv:0706.3762 [astro-ph].
- [58] A. Burrows, T. Wang, and D. Vartanyan, Channels of Stellar-mass Black Hole Formation, arXiv e-prints, arXiv:2412.07831 (2024), arXiv:2412.07831 [astro-ph.SR].
- [59] Y. Suwa, A. Harada, K. Nakazato, and K. Sumiyoshi, Analytic solutions for neutrino-light curves of core-collapse supernovae, *Progress of Theoretical and Experimental Physics* **2021**, 013E01 (2021), arXiv:2008.07070 [astro-ph.HE].
- [60] Y. Suwa, A. Harada, M. Harada, Y. Koshio, M. Mori, F. Nakanishi, K. Nakazato, K. Sumiyoshi, and R. A. Wendell, Observing Supernova Neutrino Light Curves with Super-Kamiokande. III. Extraction of Mass and Radius of Neutron Stars from Synthetic Data, *Astrophys. J.* **934**, 15 (2022), arXiv:2204.08363 [astro-ph.HE].
- [61] A. Harada, Y. Suwa, M. Harada, Y. Koshio, M. Mori, F. Nakanishi, K. Nakazato, K. Sumiyoshi, and R. A. Wendell, Observing Supernova Neutrino Light Curves with Super-Kamiokande. IV. Development of SPECIAL BLEND: A New Public Analysis Code for Supernova Neutrinos, *Astrophys. J.* **954**, 52 (2023), arXiv:2304.05437 [astro-ph.HE].
- [62] Y. Suwa, A. Harada, M. Mori, K. Nakazato, R. Akaho, M. Harada, Y. Koshio, F. Nakanishi, K. Sumiyoshi, and R. A. Wendell, Observing Supernova Neutrino Light Curves with Super-Kamiokande. V. Distance Estimation with Neutrinos, *Astrophys. J.* **980**, 117 (2025), arXiv:2404.18248 [astro-ph.HE].

- [63] A. L. Foguel and E. S. Fraga, Analytic approach to axion-like-particle emission in core-collapse supernovae, *Astroparticle Physics* **151**, 102855 (2023), arXiv:2209.14318 [hep-ph].
- [64] <https://sites.google.com/g.ecc.u-tokyo.ac.jp/nulc>.
- [65] F. A., Extended Theories of Gravity, *JHEP* **VV**, PPP, arXiv:0000.0000.